Semianalytic Modelling of a Magnetic Levitated Disk with nonuniform Polarization

S. Michael*, G. Scheinert** and H. Uhlmann **

* Institute for Microelectronic- and Mechatronic- Systems gGmbH, Langewiesener Str. 22, 98693 Ilmenau
Steffen.Michael@IMMS.de
** Dep. of Fundamentals and Theory of Electrical Engineering, Ilmenau Technical University
P. O. Box 100565, 98684 Ilmenau, GERMANY

ABSTRACT

A magnetic bearing for a high rotating electromagnetic drived disk with regard to future applications like the Laser-TV is modelled and designed. For modelling of the system consisting of permanent magnets and copper coils a semianalytic calculation tool is presented. Based on this tool it follows a static optimization of geometrical and magnetic bearing parameters. A first function model with a reached rotor speed of $48.000rpm$ validates the semianalytic model and realized investigation.

Keywords: magnetic bearing, permanent magnet

INTRODUCTION

The practical background for the design investigations of an electromagnetic levitated and drived disk was the Laser-TV, or more exactly, the laser beam deflection unit. By means of a rotating polygonal mirror the unit displayed in fig. 1 deflects the laser beam in the horizontal direction. Because of a high TV-picture quality the perspectively demanded amount of revolutions per minute is about $240,000$. This leads to the usage of a magnetic bearing with a small radial and axial displacement (less than $0.5mm$) - the application of other, e. g. mechanical bearings is not possible because of friction - and an electromagnetic drive.

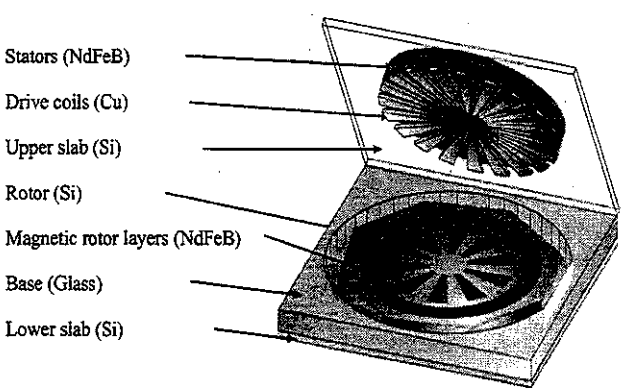

Figure 1: Structure of the laser beam deflection unit

The rotor dimension (diameter $d_r < 50mm$, height $h_r < 4mm$) seems unusually for a microsystem. The high rotor speed requires very small tolerances, furthermore copper coils embedded in silicon are stressed with the necessary current densities of $J_s = 200A/mm^2$. Due to small tolerances, physical boundary conditions, lower costs and the good possibilities of an automatic fabrication the whole arrangement should be manufactured in microsystem technologies.

Accordingly the base material for the rotor and ground plate is silicon. The ground plates are connected by a glass plate in such a way, that the rotor works in vacuum. The incident and the deflected laser beam passes through the glass plate. The permanent magnetic material is NdFeB (thickness $h \approx 0.5mm$).

BEARING STRUCTURE

Resulting from the boundary conditions an electromagnetic system should be designed in such a way, that the axial, radial and angular degree of freedom are locked, and in the remaining degree the drive performs. The bearing structure is essentially determined by the Earnshow theorem [1]. Excluding superconducting coils because of high costs or diamagnetic material (low forces) the Earnshow theorem states that the global stiffness of a magnetostatic system can not be positive. Thus at least one degree of freedom has to be locked actively with coils. Considering a single axial or radial bearing refering to the unstable degree of freedom neither the radial bearing nor the axial one leads to a satisfying solution: the acitively locked radial degree of freedom for an axial bearing is as well as the angular one for a radial bearing difficult to realize. Resulting from this consideration the bearing is composed of an inner radial and an outer axial bearing system [2]. The total radial force (F_r) of both bearing systems (radial-$_{RAD}$, axial-$_{AX}$) and the corresponding angular momentum ($M_r = F_z \cdot r$) has to fulfill the following stability conditions:

$$F_{r_{RAD}} + F_{r_{AX}} < 0 \quad \text{(Radial stab.)} \quad (1)$$

$$F_{z_{RAD}} \cdot r_{RAD} + F_{z_{AX}} \cdot r_{AX} < 0 \quad \text{(Angular stab.)} \quad (2)$$

Thus the remaining axial degree of freedom is locked actively with concentric copper coils. Dynamic problems of the actively locked axial degree like the detection of

the rotor position and the controling of the coils are not considered.

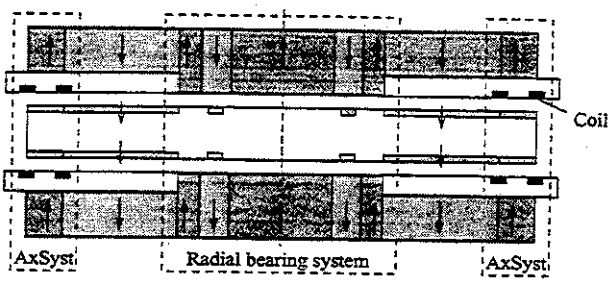

Figure 2: Principal bearing structure (AxSyst - axial bearing system)

To increase the forces each stator consists of several single opposite magnetized rings. The stators attract each other. For technological reasons all magnetic layers on the rotor surfaces are magnetized in the same direction. The planar multiphase drive is situated between the axial and radial bearing system. To realize the drive the rotor layers between both bearing systems are partially structured in the form of circle segments.

SEMIANALYTIC MODELLING

Equations for the Lorentz force (equivalent of bearing forces)

$$\mathbf{F} = I \int_L (d\mathbf{l} \times \mathbf{B}) \tag{3}$$

and resulting momentums were derived on the basis of the elementary current model [3]. Magnetic material with a constant polarization $\mathbf{J}$ can be described by equivalent torus currents. Depending on a uniform or nonuniform polarization the currents form only a current sheet on the sidings of the axial magnetized ring or they are distributed inside too.

Following equations for the flux density and Lorentz force of magnets with uniform polarization described by a single torus current are derived. Subsequently the calculation of nonuniform polarized magnets including adapted mesh generation is presented.

Magnets with Uniform Polarization

For an axially magnetized ring with the height a, the axial distance b and the radius r_0 the corresponding current I is defined as

$$I = \int_b^{a+b} \frac{\mathbf{J}}{\mu_0} dz\, \mathbf{e}_z. \tag{4}$$

A favourable way to derive the flux density is to calculate at first the magnetic vector potential $\mathbf{A}$. The curl of $\mathbf{A}$ leads then to the components of the flux density. The vector potential caused by the current I has due to existing symmetries only one component in direction ϕ. For a point P with the cylindrical coordinates $(z, r, 0)$ follows [4]:

$$\begin{aligned} A_\phi &= \frac{\mu_0 I}{4\pi} \int_0^{2\pi} \frac{r_0 \cos\alpha \, d\alpha}{\rho} \\ &= \frac{\mu_0 I r_0}{4\pi} \int_0^{2\pi} \frac{\cos\alpha \quad d\alpha}{\sqrt{(z-z_0)^2 + r_0^2 + r^2 - 2r_0 r\cos\alpha}} \end{aligned} \tag{5}$$

Due to $\mathbf{B} = \nabla \times \mathbf{A}$ the radial flux density is

$$B_r = -\frac{1}{\mu_0} \frac{\partial A_\alpha}{\partial z}, \tag{6}$$

the substitution of (4),(5) and the differentiation leads to

$$B_r = \frac{J r_0}{4\pi} \int_0^{2\pi} \int_a^{a+b} \frac{(z-z_0)\cos\alpha \qquad dz_0\, d\alpha}{\sqrt{(z-z_0)^2 + r_0^2 + r^2 - 2r_0 r\cos\alpha}^3} \tag{7}$$

The integration of z_0 results in

$$\begin{aligned} B_r &= \frac{J r_0}{4\pi} \sum_{\nu=1,2} (-1)^{\nu+1} \\ &\int_0^{2\pi} \frac{\cos\alpha \, d\alpha}{\sqrt{(z-z_\nu)^2 + r_0^2 + r^2 - 2r_0 r\cos\alpha}} \end{aligned} \tag{8}$$

with $z_1 = b$ and $z_2 = a + b$. To solve the remaining integral the substitution $\alpha = \pi - 2\beta$ is performed with regard to obtain the canonical forms of the elliptic integrals. With $\cos(\pi - 2\beta) = 2\sin^2\beta - 1$ and rewriting for the radial flux density of an axial magnetized ring follows

$$\begin{aligned} B_r &= \frac{J}{2\pi r} \sum_{\nu=1,2} (-1)^{\nu+1} \sqrt{(z-z_\nu)^2 + (r+r_0)^2} \\ &\left[\left(1 - \frac{k_\nu^2}{2}\right) K(k_\nu) - E(k_\nu) \right], \end{aligned} \tag{9}$$

$$k_\nu = \frac{4 r r_0}{(z-z_\nu)^2 + (r+r_0)^2}. \tag{10}$$

In a similar manner the axial flux density could be obtained. Executing the partial derivative of the vector potential $\mathbf{A}$ results in

$$B_z = \frac{J r_0}{4\pi} \int_0^{2\pi} \int_b^{a+b} \frac{(r_0 - r\cos\alpha)\; dz_0\, d\alpha}{\sqrt{(z-z_0)^2 + r_0^2 + r^2 - 2r_0 r\cos\alpha}^3}. \tag{11}$$

After integration in z_0 the known substitution $\alpha = \pi - 2\beta$ leads to the canonical forms of the complete elliptic integrals of the first and third kind:

$$B_z = \frac{J}{2\pi} \sum_{\nu=1,2} (-1)^\nu \frac{(z - z_\nu)}{\sqrt{(z - z_\nu)^2 + (r + r_0)^2}} \left[K(k_\nu) + \frac{r_0 - r}{r_0 + r} \Pi(n, k_\nu) \right], \quad (12)$$

$$n = \frac{4 r r_0}{(r + r_0)^2}. \quad (13)$$

For computing the flux density of control coils (used for the actively locked axial degree of freedom) (4) is to substitute by

$$I = \int_0^{a_s} I_s w \, dz \quad (14)$$

(I_s - current sheet, w - number of windings, a_s - thickness), which results in similar equations for the components of the flux density like (9),(12).

The flux density $\mathbf{B}$ and the current I of (3) are determined. Due to thin rotor magnet layers a useful approximation is perfomed; the integration over the thickness z_R in (4) is substituted by

$$I = \frac{\mathbf{J}}{\mu_0} z_R \, \mathbf{e}_z. \quad (15)$$

The remaining integration of the vector product of I and $\mathbf{B}$ to obtain the Lorentz force is performed numerically. The force calculation of a radial displaced rotor requires the introduction of a second cylindrical coordinate system (r^*, phi^*, z^*) for the rotor (the origin is identical with the rotor centre of gravity). For the bearing force follows (r_R-radius of the rotor magnet)

$$\mathbf{F} = \frac{J}{\mu_0} z_R^* r_R^* \left[\overline{e_r} \int_0^{2\pi} B_z^* d\alpha^* - \overline{e_z} \int_0^{2\pi} B_r^* d\alpha^* \right] \quad (16)$$

Momentums are calculated in an analogue way.

In case of no angular displacement the expendable numerical integration could be avoided by an approximation. Picking exemplary the radial force (Δr-radial rotor displacement)

$$F_r = \frac{J}{\mu_0} z_R^* r_R^* \int_0^{2\pi} B_z^*(r(\Delta r, r_R, \alpha^*)) \, d\alpha^*, \quad (17)$$

a polynom of second order approximates the axial flux density component:

$$B_z^* = a_0 + a_1 r + a_2 r^2 \quad (18)$$

The coefficients a_0, a_1, a_2 are determined by the least square method. Substituting (18) in (6) leads to the expression

$$F_r = c_0 \, r_R \Big(2a_0 + 2/3 a_1 \frac{(r + \Delta r)}{m} E(m) + 4a_2 (r + \Delta r)^2 (\pi/2 - m) \Big) \quad \text{with} \quad (19)$$

$$r = 2(\Delta r + r_R)\sqrt{1 - k \sin \beta^2} \quad \text{and} \quad (20)$$

$$m = \frac{4 r \Delta r}{(r + \Delta r)^2}. \quad (21)$$

Nonuniform Magnetization

The flux density components for magnetic material with a constant polarization were obtained above. For modelling a nonuniform polarized ring this one is divided into finite subrings with constant polarization. The material equation

$$\mathbf{B} = \mu \mathbf{H} + \mathbf{J} \quad (22)$$

shows after rewriting the linear dependency of the polarization from the outer magnetic field:

$$\mathbf{J} = (\mu_r - 1)\mathbf{B} + \mathbf{J}_s. \quad (23)$$

To determine the polarization of each subring a linear equation system is to solve. Referring to (12) the axial flux density is given by

$$B_z = J_i \, g_i(r, z) \quad \text{with} \quad (24)$$

$$g_i(r, z) = \frac{1}{2\pi} \sum_{\nu=1,2} (-1)^\nu \frac{(z - z_\nu)}{\sqrt{(z - z_\nu)^2 + (r + r_0)^2}} \left[K(k_\nu) + \frac{r_0 - r}{r_0 + r} \Pi(n, k_\nu) \right]. \quad (25)$$

Applying (23) for all n subdomains yields the equation system

$$\begin{pmatrix} 1 & + \cdots + f_n(r_1, z_1) \\ f_1(r_2, z_2) & + \cdots + f_n(r_2, z_2) \\ \cdots & \cdots \\ f_1(r_m, z_m) & + \cdots + 1 \end{pmatrix} \bullet \begin{pmatrix} J_1 \\ J_2 \\ .. \\ J_n \end{pmatrix} = J_s \quad (26)$$

with $f_i(r, z) = (\mu_r - 1) \cdot g_i(r, z)$ and the saturation polarization J_s. The equation system has no anomalies and is solved directly.

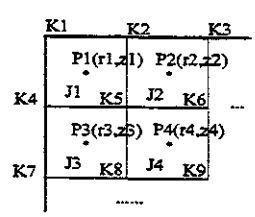

Figure 3: Detail of the meshed ring

Considering the equation system structure regarding to typical values of the relative permeability ($\mu_r \simeq 1$) an equidistant mesh is not usefull. Due to the small relative permeability values and small flux density changes inner adjacent elementary currents annul often each other. Therefore an adapted mesh conforming the polarization is generated by an iterative algorithm. Starting with a uniform magnetization the flux density is examined in the default equidistant meshed ring. Is

$$\sum_i (B_z(r_i, z_i) - \sum_i B_z(r_i, z_i)) \quad < \quad \epsilon \qquad (27)$$

(i- adjacent node elements) valid for a given ϵ the correspondig node is deleted. The algorithm converges after the first step and leads to a reduction of the matrix dimension about 50 percent at the same accuracy.

The bearing force results finally by superposition of all partial forces and flux densities. Finally the semianalytic model is implemented in a software tool with a front- and backend to the program *matlab*.

Results of Simulation

Applying the semianalytic tool to an example, a single ring magnet ($\mu_r = 1.04$, $J_s = 1.175T$), fig. 4 shows the expected flux density field with a nearly constant axial flux density component inside the magnet and an expanding of the flux density on the border.

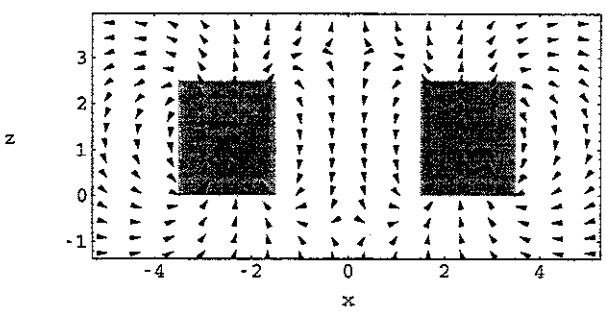

Figure 4: Vector field of **B** from the gray colored ring magnet ($r - z$ level)

Regarding the flux density field and the corresponding polarization (fig. 5) the correlation can observed. The nearly constant axial flux density component inside the magnet and the low value of the relative permeability causes low changes of the polarization ($J_{min} = 1.15, J_{max} = 1.173$). A Comparison of nonuniform and uniform polarized magnets leads to force differences about only ten percent (referring to an arrangement of two single magnets). For the bearing structure such differences are not neglectable, because the resulting deviation of the bearing force as the difference between the forces of axial and radial bearing system could be up to 100 percent.

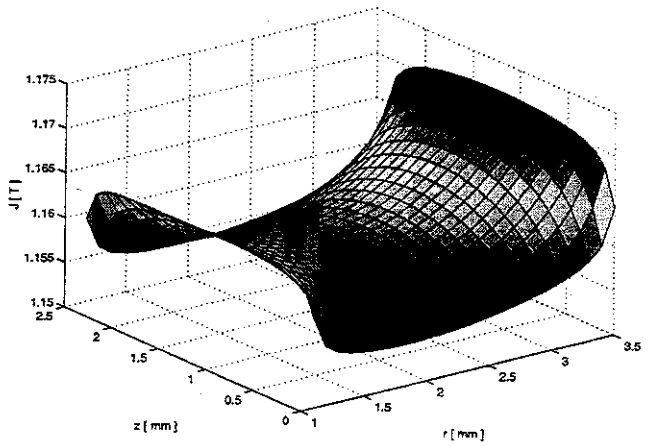

Figure 5: Polarization J inside the magnet versus radial (r) and axial (z) dimension ($\mu_r = 1.04$)

Based on the model the bearing system is designed. To determine the geometrical parameters a static optimization is performed [5]. The optimization has several conditions like the functionality of the drive and a maximal axial, radial and angular stiffness (which should be received by a minimal coil current). The conditions interact each other and have to be weighted regarding to the stability conditions. As an example the calculated radial force is shown in figure 6 – the locking of the degree of freedom is obviously because of the negative reaction force in the whole area of radial and axial displacement.

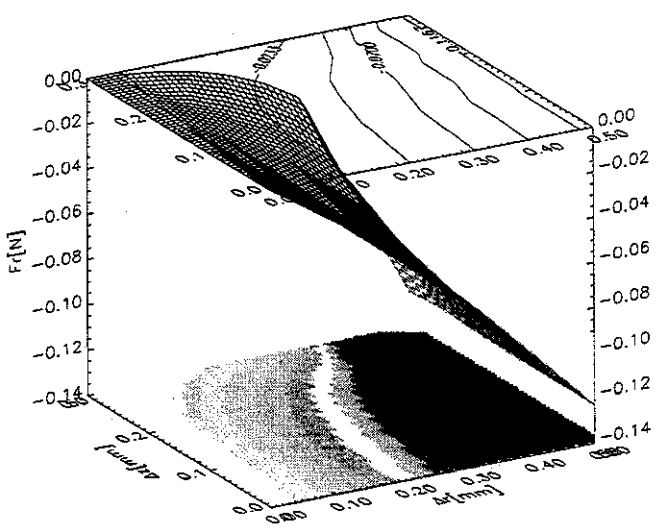

Figure 6: Radial force F_r versus radial (Δr) and axial (Δz) displacement

EXPERIMENTAL STUDY

Flux density and force measurements were performed on a three-dimensional prototype. Reasoned in technological problems the prototype is fabricated still in microsystem technologies and precision engineering too. For instance the coils which are manufactured in printed circuit board technologies with the result of a lower maximum current density.

A concentric faseroptic sensor detects the axial rotor displacement and yields the PID controller input signal. The current of the axial control coils is the analogue amplified controller output signal [].

Passive magnetic bearings effects in the locked degree of freedom a stiffness, but no damping. First investigation for a future electromagnetic rotor damping are performed. The damping of the prototype is realized by a 2-mass-swinger in such a way, that the unit is connected with the chassis about damping elements.

Several model verifications were realized which showed the principal correctness of the semianalytic formulas. Fig. 7 shows measured values of the axial flux density component. Calculated and measured values have a good concordance (deviation less than 3%). The exact polarization of the magnetized rings is not known therefore the polarization is calibrated on measured values.

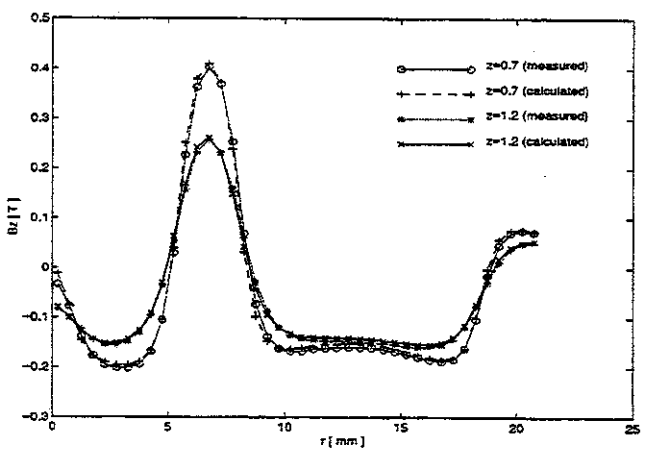

Figure 7: Simulated and measured B_z-values of the stator versus different axial distances $(z_0 = 0.7mm, z_1 = 1.2mm)$

The maximal measured deviations about 20 percent from the computed activ axial forces (fig. 8) are caused by large geometrical tolerances and a nonuniform (measured) polarization amplitude around the stator.

The rotor of the function prototype reached a speed of $48.000rpm$. At this speed a radial instability occurs

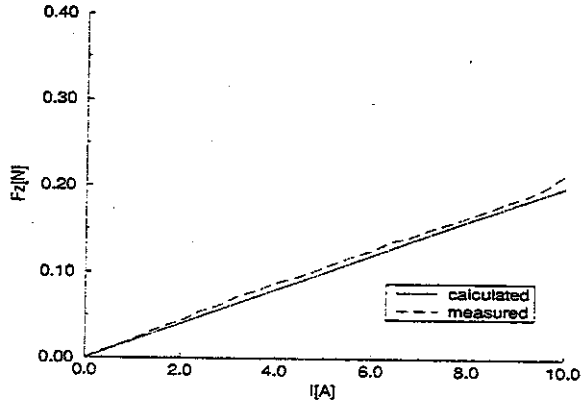

Figure 8: Measured and calculated activ axial force versus current I of control coils

whose reasons are the subject of the present investigation. In this context the influence of magnetic tolerances and the interaction between bearing and drive are examined.

CONCLUSION

A semianalytic calculation tool for modelling of magnetic bearings has been presented. Due to the performance the tool is well suited for parameter studies and optimizations. Based on the developed tool a magnetic bearing was designed and simulated. A first prototype showed the principal correctness of the modelling. Stability problems in higher speed regions are the subject of further investigation.

REFERENCES

1. S. Earnshow: "On the Nature of the Molecular Forces which regulate the Constitution of the Luminiferous Ether."; Camb. Phil. Soc., N. VII/1, S. 97-112, 1839
2. J. Delamare, J. P. Yonnet, E. Rullière: "A Compact Magnetic Suspension With Only One Axis Control"; IEEE Transactions on Magnetics, Vol. 30, No. 6, Nov. 1994
3. H. Hoffmann: "Das elektromagnetische Feld"; Springer, Wien 1982
4. K. Simonyi: "Theoretische Elektrotechnik"; Dt. Verlag der Wissenschaften, Berlin 1971

5 A. Albrecht, S. Michael, G. Scheinert: "Simulation and Optimization of a Magnetic Levitated Disk"; Microsystem Technologies 1996; Springer, Berlin 1996